# Intracellular Proton Regulation of ClC-0

Giovanni Zifarelli, Anna Rosa Murgia, Paolo Soliani, and Michael Pusch

Istituto di Biofisica, Consiglio Nazionale delle Ricerche, I-16149 Genova, Italy

Some CLC proteins function as passive $Cl^-$ ion channels whereas others are secondary active chloride/proton antiporters. Voltage-dependent gating of the model *Torpedo* channel ClC-0 is modulated by intracellular and extracellular pH, possibly reflecting a mechanistic relationship with the chloride/proton coupling of CLC antiporters. We used inside-out patch clamp measurements and mutagenesis to explore the dependence of the fast gating mechanism of ClC-0 on intracellular pH and to identify the putative intracellular proton acceptor(s). Among the tested residues (S123, K129, R133, K149, E166, F214L, S224, E226, V227, C229, R305, R312, C415, H472, F418, V419, P420, and Y512) only mutants of E166, F214, and F418 qualitatively changed the $pH_{int}$ dependence. No tested amino acid emerged as a valid candidate for being a pH sensor. A detailed kinetic analysis of the dependence of fast gate relaxations on $pH_{int}$ and $[Cl^-]_{int}$ provided quantitative constraints on possible mechanistic models of gating. In one particular model, a proton is generated by the dissociation of a water molecule in an intrapore chloride ion binding site. The proton is delivered to the side chain of E166 leading to the opening of the channel, while the hydroxyl ion is stabilized in the internal/central anion binding site. Deuterium isotope effects confirm that proton transfer is rate limiting for fast gate opening and that channel closure depends mostly on the concentration of $OH^-$ ions. The gating model is in natural agreement with the finding that only the closing rate constant, but not the opening rate constant, depends on $pH_{int}$ and $[Cl^-]_{int}$.

The Journal of General Physiology

## INTRODUCTION

ClC-0 can be considered the founding member of the CLC protein family as it was the first CLC to be functionally characterized and cloned (Miller and White, 1980; Jentsch et al., 1990). The CLC protein family comprises both chloride channels and chloride/proton antiporters (Accardi et al., 2004; Picollo and Pusch, 2005; Scheel et al., 2005; Zifarelli and Pusch, 2007; Jentsch, 2008) that, in spite of their different thermodynamic control of $Cl^-$ movement, share a significant degree of homology and a very similar architecture (Chen et al., 2003; Estévez et al., 2003; Engh and Maduke, 2005). They are all dimers composed of two identical subunits each containing an ion conduction pathway (Dutzler et al., 2002). Several human CLC proteins and associated β subunits are involved in human genetic diseases, underscoring their physiological relevance (Jentsch et al., 2005a,b; Jentsch, 2008).

Due to various favorable properties, ClC-0 has served as a model to explore the mechanisms of gating and permeation for all CLC channels (Jentsch et al., 2002; Chen, 2005; Matulef and Maduke, 2007; Zifarelli and Pusch, 2007). The conducting state of ClC-0 is determined by the operation of two gating mechanisms: a common gate, controlling opening and closing of the two pores simultaneously, and a protopore gate, acting individually on each pore (Chen, 2005; Zifarelli and Pusch, 2007). The operation of the fast gate depends on voltage and $H^+$ and $Cl^-$ concentrations on both the intracellular and extracellular side (Pusch, 2004; Chen, 2005). In particular, external pH and $[Cl^-]$ influence the opening rate without affecting the closing rate (Pusch et al., 1995; Chen and Miller, 1996; Pusch, 1996; Ludewig et al., 1997a; Chen and Chen, 2001, 2003), whereas intracellularly, $Cl^-$ affects mostly the closing rate (Chen and Miller, 1996). The origin of the asymmetrical dependence on extracellular and intracellular factors is still unknown. Structural analysis of the bacterial ClC-ec1 has suggested that in the closed conformation, the side chain of E148 (corresponding to E166 in ClC-0) directly occludes the ion permeation pathway, whereas upon mutation of this residue to alanine or glutamine, a $Cl^-$ ion was found at the site occupied by the side chain of E148 (Dutzler et al., 2002, 2003). In particular, the structure of the mutant E148Q showed that the side chain of the glutamine is directed away from the pore toward the extracellular side. It was therefore hypothesized that this represents the conformation of the WT protein in the open state (Dutzler et al., 2003).

These structural results suggested a specific role of this conserved glutamate in the fast gating mechanism of ClC-0, even though ClC-ec1 is a $Cl^-/H^+$ antiporter, whereas ClC-0 is a $Cl^-$ channel. This interpretation was confirmed by electrophysiological investigations of the mutants E166A, E166V, and E166Q of ClC-0 that displayed an open, voltage-independent phenotype,

Correspondence to Michael Pusch: pusch@ge.ibf.cnr.it

The online version of this article contains supplemental material.

Abbreviation used in this paper: CPA, p-chloro-phenoxy-acetic acid.


The Rockefeller University Press $30.00
J. Gen. Physiol. Vol. 132 No. 1 185–198
www.jgp.org/cgi/doi/10.1085/jgp.200809999

proving that the neutralization of the side chain of the E166 eliminated the fast gating process (Dutzler et al., 2003; Traverso et al., 2003, 2006). Moreover, the phenotype of WT ClC-0 at low extracellular pH resembled that of the mutants of E166 in which the carboxylate side chain was practically absent (E166A) or its charge was neutralized (E166Q) (Chen and Chen, 2001; Dutzler et al., 2003). These data have been interpreted in terms of a protonation-dependent displacement of the side chain of E166 leading to channel opening; upon protonation from the outside, E166 moves from the blocking position to a position displaced from the pore (without any other conformational changes). Such an interpretation suggests potentially significant similarities in the mechanism of external $H^+$ regulation for ClC-ec1 and ClC-0. Moreover, this model provides a possible mechanism to explain the effect of external $Cl^-$ on the fast gate; $[Cl^-]_{ext}$ would increase the opening rate, competing with the side chain of E166. However, this scenario cannot fully explain the very different effect of $[Cl^-]_{int}$.

In spite of this progress, the molecular mechanism of gating of ClC-0 is still very poorly understood. First of all, several pieces of evidence suggest that the fast gate can open by different molecular routes. This has first been described by Chen and Miller (1996) who found a biphasic dependence of the opening rate, α, on voltage. α increases exponentially at positive voltages, reflecting the major voltage-dependent opening step ("route 1"). However, after passing through a minimum, α increases also at negative voltages, reflecting a different route of opening that leads to the significant residual open probability seen at negative voltages ("route 2") (Chen and Miller, 1996). It is mainly the latter pathway of opening that is affected by extracellular pH, whereas the major voltage-dependent opening step (route 1) is relatively independent from $pH_{ext}$ (Chen and Chen, 2001) but is influenced by $[Cl^-]_{ext}$. The very different nature of these two routes to channel opening is even more extreme in the point mutant E166D. For this mutant, the open state favored by low external pH (route 2) has a smaller single channel conductance than the one reached by the major voltage-dependent route 1 (Traverso et al., 2006). Intracellular pH appears to act on the voltage dependence of channel closing and on the voltage-dependent part of channel opening (route 1). Early experiments by Hanke and Miller demonstrated that changes of $pH_{int}$ lead to a shift of the voltage dependence of the open probability of ClC-0 reconstituted in lipid bilayers (Hanke and Miller, 1983). Similar effects have been described for the muscle channel ClC-1 expressed in Sf-9 cells (Rychkov et al., 1997). Recently, our group investigated the dependence of the ClC-0 mutant E166D on $pH_{int}$ (Traverso et al., 2006). Similar to the results of Hanke and Miller we found that lowering $pH_{int}$ leads to a shift of the voltage-dependent part of the open probability to more negative voltages. Our results were consistent with the idea that the major voltage-dependent step of the opening reflects the protonation of E166/D166 from the intracellular side. In this model, protons could reach this position directly from the intracellular solution or they could be shuttled via one or more intermediate protonatable groups. In the latter case, a key protonatable group, the $H^+$ sensor, mediates the effects of $pH_{int}$. A contribution of protons to voltage-dependent gating has been also recently proposed by Miller (2006).

In alternative, intracellular protons might modulate another voltage-dependent step, as originally suggested by Hanke and Miller (1983).

In this respect it must be taken into account that we have proposed that fast gating of ClC-0, beside a movement of the side chain of E166, additionally involves conformational changes in the channel pore (Accardi and Pusch, 2003; Traverso et al., 2003). Moreover, it has been suggested that the displacement of the side chain of E166 upon channel opening might be directed toward the internal rather than the external side of the channel (Bisset et al., 2005). The investigation of the molecular determinants of the sensitivity to intracellular $H^+$ has been pursued only for ClC-ec1 and has led to the identification of E203, which is conserved among CLC transporters but not CLC channels. The mutation E203Q completely abolished proton transport but preserved $Cl^-$ transport, similar to the E148A mutant (Accardi et al., 2005). However, at variance with the E148A mutant, E203Q does not suppress the proton sensitivity of the remaining $Cl^-$ currents (Accardi et al., 2005). An important role for proton transport of the corresponding glutamate was also confirmed in ClC-4 and ClC-5 (Zdebik et al., 2008). In the present study we intend to investigate in detail the mechanism of intracellular proton regulation of the fast gate of ClC-0 and to identify amino acid residues that are involved in this process. We were not able to identify any specific intracellular proton acceptor. However, based on kinetic analysis and deuterium isotope effects, we propose a gating model in which the proton required for channel opening originates from the dissociation of an intrapore water molecule. The resulting $OH^-$ anion is possibly stabilized in the channel pore by one of the channel's anion binding sites.

## MATERIALS AND METHODS

### Molecular Biology and Oocyte Expression

WT ClC-0 and all mutants were in the PTLN vector (Lorenz et al., 1996). We used the C212S mutant that eliminates the slow, common gate (Lin et al., 1999) as the basis for most constructs, except where explicitly stated. Mutations were introduced by oligonucleotide-directed mutagenesis using Pfu polymerase (Fermentas). The PCR-generated regions were fully sequenced. RNA

was prepared using the mMessage mMachine SP6 kit (Ambion) and injected into *Xenopus* oocytes as previously described (Pusch et al., 2000).

### Electrophysiology

Currents were recorded using the two-electrode voltage-clamp method and excised patch-clamp recording as previously described (Ludewig et al., 1997b; Pusch et al., 2000). For whole oocyte voltage clamp measurements, the bath solution contained (in mM) 100 NaCl, 4 $MgSO_4$, 5 HEPES, pH 7.3, and the holding potential was chosen close to the resting membrane potential (−30 to −50 mV). For patch clamping, the intracellular solution contained (in mM) 100 NMDG-Cl or 100 NaCl, 2 $MgCl_2$, 10 HEPES, 2 EGTA, pH 7.3, whereas the standard extracellular solution contained 100 NMDG-Cl, 5 $MgCl_2$, 10 HEPES, pH 7.3. HEPES was substituted by MES for solutions with 5 < pH < 6.5, bis-tris-propane for solutions with 8 < pH < 9, and glutamate for solutions with pH < 6, Na-borate or CAPS for solution with pH 10. For measurements at low $[Cl^-]$ in the internal solution, 90 mM NMDG-Cl was substituted with equimolar amounts of Na-glutamate, and the reference electrode was connected to the bath by an agar bridge.

For measurements in $D_2O$, solutions were prepared with NaCl (extracellular and intracellular) instead of NMDG-Cl in order to minimize the presence of $H^+$ due to the titration of NMDG with HCl. As an internal control, for each patch in which we tested the effect of intracellular $D_2O$, we also performed registrations in solutions prepared with $H_2O$, in which for consistency we also used NaCl instead of NMDG-Cl. To determine the pH (pD) of the solutions prepared with $D_2O$ we added 0.4 pH units to the pH meter reading (Glasoe and Long, 1960; DeCoursey and Cherny, 1997). All substances were purchased from Sigma-Aldrich. $D_2O$ was 99.9 atom percent D.

Solutions in patch-clamp experiments were changed by inserting the patch pipette into perfusion tubes of 0.5 mm diameter. The voltage protocol for patch clamping consisted of a prepulse to 80 mV followed by a test pulse to variable potentials (from 140 to −160 mV) (standard duration 100 ms) in 20-mV increments and a step to −140 mV.

To study more closely the activation process, the protocol consisted of a prepulse to −140 mV (50 ms) followed by a test pulse to variable potentials (from 160 to −140 mV) in 20-mV increments and a step to −140 mV (50 ms). To study more closely the deactivation process, the protocol consisted of a prepulse to 100 mV (20 ms) followed by a test pulse to variable potentials (from −180 to 120 mV) in 20-mV increments and a step to −140 mV (50 ms).

Patch-clamp data were recorded using an EPC-7 amplifier (HEKA) and the custom acquisition program (GePulse) (the acquisition program is available at http://www.ge.cnr.it/ICB/conti_moran_pusch/programs-pusch/software-mik.htm). The holding potential in patch clamp measurements was 0 mV. Voltage clamp measurements employed an NPI-TEC 05 amplifier (NPI Electronics), and were performed as described previously (Traverso et al., 2003). Data analysis was performed using custom software (written in Visual C++, Microsoft), the Origin program (OriginLab Corporation), and SigmaPlot (SPSS Inc.). Capacitive transients in patch clamp experiments were often removed using appropriately scaled responses to voltage steps to 0 mV (in standard solutions) or steps to the reversal potential (in low chloride solutions).

Unless otherwise stated, open probabilities were derived from the tail currents by fitting a modified Boltzmann function:

$$I(V) = I_{max}(p_{min} + (1 - p_{min})/(1 + exp[z(V_{1/2} - V)F/(RT)])), \quad (1)$$

where $I_{max}$ is the (fitted) maximal current, $p_{min}$ the residual open probability at negative voltages, $V_{1/2}$ is the midpoint voltage of the open probability, z the apparent gating valence, F the Faraday constant, R the gas constant, and T the absolute temperature.

### Online Supplemental Material

We provide supplemental material (available at http://www.jgp.org/cgi/content/full/jgp.200809999/DC1) describing the phenotype of the following mutants: C212S/K129A, C212S/H472K, C212S/E226Q, F214L, and C212S/F418A.

## RESULTS

### Dependence of WT $p_{open}$ on Internal pH

Fig. 1 A shows representative macroscopic currents recorded at pH 7.3 from the ClC-0 mutant C212S, for which the common gate is constitutively open (Lin et al., 1999). Currents display the typical deactivation at negative voltages. From the initial tail currents to −140 mV the activation curve can be constructed (Fig. 1 F, open circles). The data points were fitted with Eq. 1 in order to extract three parameters that describe the voltage dependence of gating: $p_{min}$, the minimum open probability at most negative voltages; $V_{1/2}$, the voltage of half maximal activation; and z, the apparent gating valence. Lowering the internal pH (from now on referred to simply as pH) to 6.3, dramatically activates the currents at negative voltages (Fig. 1 B). The resulting activation curve is shifted to more negative voltages, but the fit of Eq. 1 does not provide accurate values for the gating parameters. On the other hand, intracellular alkalinization (pH 8.3, Fig. 1 C; pH 9, Fig. 1 D; pH 10, Fig. 1 E) shifts the activation curve to more positive voltages (Fig. 1, F and G). At pH 10, the deactivation of currents at negative voltages was difficult to resolve reliably for all patches. In addition, whereas the maximal current amplitude at the most positive voltages was roughly similar at pH 7.3, 8.3, and 9, maximal currents were reduced at pH 10, as is best seen in Fig. 1 G, where the steady-state IVs are superimposed. To test whether this reduction seen at pH 10 simply reflects a dramatic "shift" of the $p_{open}$, we fitted the steady-state IV with the following equation:

$$I(V) = G(V - E_{rev})\left(p_{min} + \frac{1 - p_{min}}{1 + \exp(-z(V - V_{1/2})F/(RT))}\right), \quad (2)$$

where G is the (maximal) conductance and $E_{rev}$ the current reversal potential. Fits of Eq. 2 are shown in Fig. 1 G as solid lines. The gating parameters obtained for the currents at pH 7.3, 8.3, and 9 are similar to those obtained using the tail current analysis (see legend of Fig. 1). We thus used Eq. 2 routinely also at pH < 10 for patches that showed relatively low expression. In these cases, the steady-state current evaluated from the mean of many

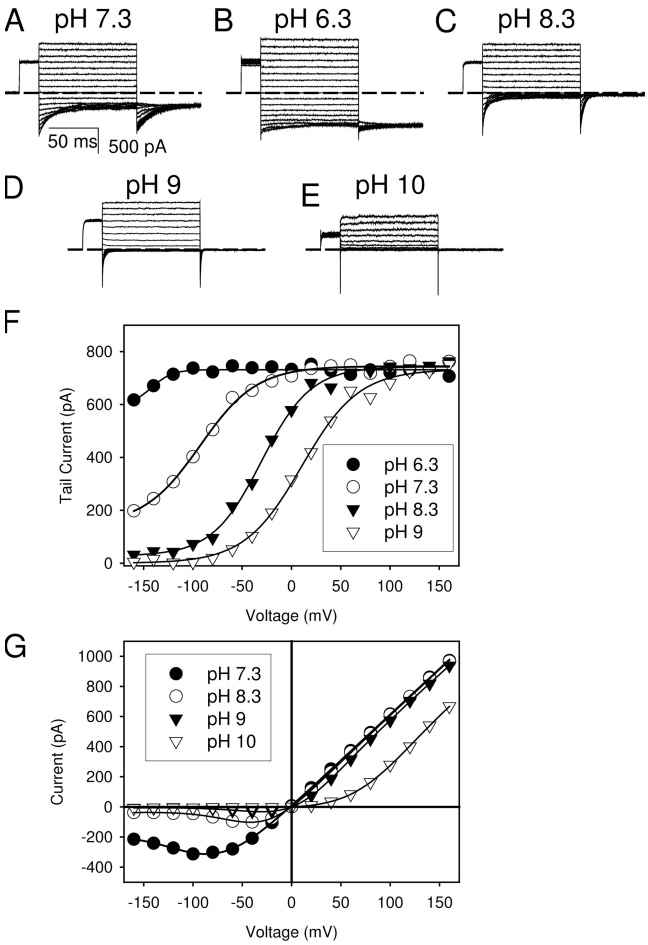


**Figure 1.** Internal pH dependence of ClC-0 fast gating. The figure illustrates the pH dependence of raw currents (A–E) and the analysis performed to extract the gating parameters (F and G). All data are from one patch expressing the C212S mutant. The symbols in F represent the (absolute values of the) initial tail currents at the tail pulse to −140 mV plotted as a function of the test pulse voltage. The symbols in G are the steady-state currents measured at the end of the test pulse. Lines in F are fits of Eq. 1 with the following parameters: pH 6.3, $V_{1/2}$ = −142 mV, z = 1.9, $p_{min}$ = 0.81; pH 7.3, $V_{1/2}$ = −93 mV, z = 0.87, $p_{min}$ = 0.19; pH 8.3, $V_{1/2}$ = −30 mV, z = 0.99, $p_{min}$ = 0.04; pH 9, $V_{1/2}$ = 10 mV, z = 0.87, $p_{min}$ = 0. Lines in G are fits of Eq. 2 with the following parameters: pH 7.3, G = 6.1 nS, $V_{1/2}$ = −91 mV, z = 0.85, $p_{min}$ = 0.15; pH 8.3, G = 6.1 nS, $V_{1/2}$ = −31 mV, z = 1.08, $p_{min}$ = 0.04; pH 9, G = 5.9 nS, $V_{1/2}$ = 7 mV, z = 1.04, $p_{min}$ = 0.004; pH 10, G = 4.6 nS, $V_{1/2}$ = 88 mV, z = 0.77, $p_{min}$ = 0.008.

data points at the end of the test pulse provides a much more robust measurement than the extrapolated initial tail current. The $V_{1/2}$ value obtained for the currents at pH 10 was significantly larger than that at pH 9.0 (see legend of Fig. 1). However, the conductance G (Eq. 2) was also reduced at alkaline pH (at pH 10, the conductance was only 76% of that at pH 7.3). Thus, the reduction of currents seen at pH 10 does not reflect a simple shift of the voltage dependence. We did not investigate in further detail the reduction of the maximal conductance at alkaline pH but concentrated on the parameters that describe the voltage dependence of gating ($p_{min}$, $V_{1/2}$, z). For pH values ≥8.3 the minimum open probability, $p_{min}$, was very small and difficult to distinguish from small leak currents. We therefore further restricted our attention to the values obtained for $V_{1/2}$ and the apparent gating valence, z. In particular, z was found to be practically independent of pH (z = 0.89 ± 0.11). The mean values obtained for $V_{1/2}$ are plotted in Fig. 2 as a function of pH. The pH dependence can be well described by a straight line with a slope of around 46 mV per pH unit, corresponding to around 20 mV per e-fold change of the $H^+$ concentration.

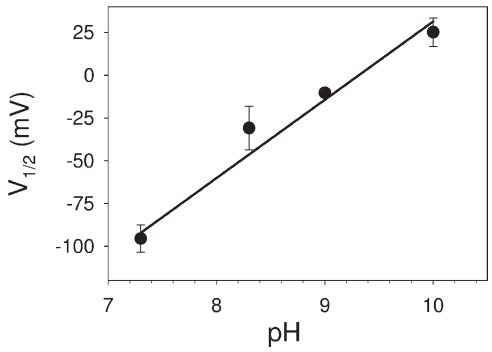


**Figure 2.** Dependence of the voltage of half-maximal activation on internal pH. Mean values of $V_{1/2}$ are plotted as a function of pH. Error bars indicate SD. The straight line has a slope of 46 ± 2 mV per pH unit, corresponding to 20 mV per e-fold change of the $H^+$ concentration.

## Mutational Analysis

To find out if the pH effects are mediated by a protonatable group that acts as a $H^+$ sensor, we performed a mutagenic screen of several residues indicated in Fig. 3 along with their localization in the secondary structure of the channel.

The residues to be mutated were chosen according to several criteria. Most of them are predicted to be accessible to the intracellular solution, according to the structure of the bacterial homologue ClC-ec1 (Dutzler et al., 2002). The residues S123, F418, and Y512 are critical in the coordination of $Cl^-$ at the central binding site and V419 and P420 might also indirectly influence the site occupancy. The residue K149, although not directly accessible to the intracellular solution, has been shown to influence the electrostatic milieu in the intracellular part of the ion permeation pathway (Zhang et al., 2006), and its mutation drastically alters fast gating (Zhang et al., 2006; Engh et al., 2007b). E127 and K519 are known to alter the pore conductance and fast gating properties respectively and to interact with each other (Pusch et al., 1995; Chen and Chen, 2003; Lin and Chen, 2003). Moreover, the residue E166 is known to alter the sensitivity to external pH of ClC-0 (Dutzler et al., 2003), whereas V227 is corresponding to E203 of ClC-ec1, which was found to be the intracellular acceptor

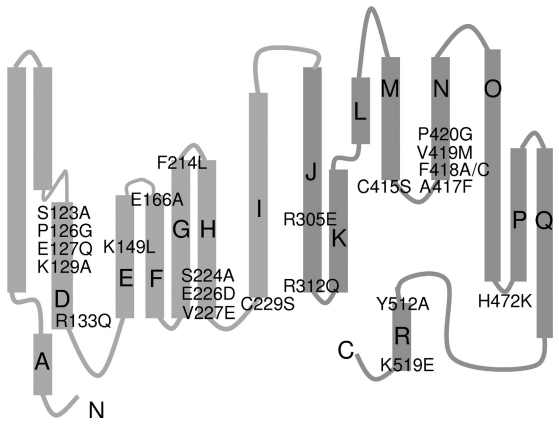


**Figure 3.** Indication of the mutated amino acids on a topological model of ClC-0 based on the crystal structure of ClC-ec1 (Dutzler et al., 2002).

of protons (Accardi et al., 2005). S224 and E226 were selected for their proximity to V227. It has been reported that aromatic residues can interact with protons through cation/π interactions (Adam et al., 2007). F214 (in the structure of ClC-ec1) is located between E226 and E166 and therefore could be involved in proton sensitivity. Together with the additional selected residues K129, R133, C229, R305, R312, C415, and H472 we covered all residues that appear to be interesting candidates for being directly protonatable sites or residues that may affect pH sensing by altering a nearby pH sensor.

Three mutants yielded only small currents: C212S/K129A, C212S/E226Q, and C212S/H472K. However, in two-electrode voltage clamp recordings, C212S/K129A and C212S/H472K showed qualitatively a similar voltage dependence and kinetics of gating as WT ClC-0 (Fig. S1, available at http://www.jgp.org/cgi/content/full/jgp.200809999/DC1), suggesting that neither H472 nor K129 are involved in pH sensing of the fast gate of ClC-0. Mutations of E226 to A, C, or T did not yield functional currents, whereas the charge-conserving mutant E226D was very similar to WT (Table I). However, the E226Q mutation yielded small currents that were quite different from WT (Fig. S2). Even though the mutant had a drastic effect on fast gating, the overall pH dependence was qualitatively similar to WT (see legend of Fig. S2). Interestingly, the slope of the pH dependence of $V_{1/2}$ is significantly larger than that of WT (155 mV per pH unit for E226Q compared with 46 mV for WT). However, the apparent gating valence of the mutant is significantly smaller (0.40 compared with 0.89 of the WT). As discussed in detail by Boccaccio et al. (1998), the larger slope of the $V_{1/2}$ versus pH curve most likely reflects an indirect effect of the reduced gating charge. To take into account the interdependence of the slope of the $V_{1/2}$ − pH curve and the gating valence, z, we also evaluated the product between them (Table I, column 5) that shows little change compared with WT for any of the mutants. We can thus conclude that E226 is not strictly essential for the pH dependence of the fast gate of ClC-0.

Among the mutations that showed robust expression and that could thus be reliably measured using the inside-out configuration, most resulted in channels with only relatively small quantitative changes in the $pH_{int}$ dependence of gating (Table I). The only three mutants that showed a drastically altered dependence on $pH_{int}$ were E166A, F214L and F418A. Even though the pH dependence of the fast gate of mutant F214L appears to be altered for pH < 9, the mutant displays the typical acceleration of deactivation at more alkaline pH, and for pH > 9 also the pH dependence of $V_{1/2}$ appears to be normal (see Fig. S3).

The other mutant that displayed an altered pH response was F418A. First of all, the mutation by itself drastically altered the fast gating process in a way similar to the homologous mutation in ClC-1 (Estévez et al., 2003); F418A, at pH 7.3, shows a pronounced slow down in the kinetics of relaxation at negative voltages compared with WT (Fig. S4). Surprisingly, in contrast to what is observed for WT ClC-0, at acidic pH (5.3), the current amplitude decreases (Fig. S4). Currents also decreased at alkaline pH, leading to an overall biphasic pH dependence (Fig. S4).

At pH 7.3, E166A presents an open channel phenotype, with almost no gating transitions, in agreement with previous studies (Dutzler et al., 2003; Traverso et al., 2003). Moreover, it was insensitive to changes in pH for values ranging from 6.3 to 8.3 (unpublished data). This behavior is expected because E166A is a constitutively opened channel on which pH can probably have no further effect. This result is also consistent with the hypothesis that opening of WT ClC-0 requires the protonation of E166, either from the outside (Dutzler et al., 2003) or from the inside (Miller, 2006; Traverso et al., 2006).

Somewhat surprisingly, E166A-mediated currents were inhibited in a voltage-dependent manner at pH ≥ 9 (Fig. 4). Currents decreased in a time-dependent manner at negative voltages, similar to the regular fast gate, but also similar to the voltage-dependent block by p-chlorophenoxy-acetic acid (CPA) (Traverso et al., 2003). To rule out that this behavior reflects a voltage-dependent block by the buffer used, we tested different buffer concentrations (1 and 10 mM) with no apparent difference in current decrease (unpublished data).

In principle, this behavior could be due to a drastic alteration of the pH sensitivity in the E166A mutant such that pH effects on gating become visible only at very alkaline pH.

However, an alternative interpretation could be that the reduction of E166A-mediated currents seen at pH ≥ 9 and at negative voltages reflects a voltage-dependent

TABLE I

*Summary of Voltage and pH Dependence of Mutants*

| Mutant | $V_{1/2}$ (mV) at pH 7.3 | Slope (mV per pH unit) | z | Slope*z/58 mV |
|---|---|---|---|---|
| C212S | −92 ± 16 | 46 ± 2 | 0.89 ± 0.11 | 0.71 |
| S123A | −105 ± 20 | 44 ± 12 | 0.78 ± 0.15 | 0.60 |
| P126G | −117 ± 4 | 45 ± 7 | 0.93 ± 0.14 | 0.72 |
| E127Q | −93 ± 13 | 66 ± 7 | 1.09 ± 0.10 | 1.25 |
| K129A | ND | ND | ND | ND |
| R133Q | −93.3 ± 8 | 63.8 ± 7 | 1.0 ± 0.16 | 1.09 |
| K149L | −45 ± 8 | 106 ± 4 | 0.69 ± 0.14 | 1.28 |
| E166A | ND | ND | ND | ND |
| F214L | 49 ± 7 | 43 ± 1 | 1.28 ± 0.04 | 0.95 |
| S224A | −105 ± 16 | 50 ± 6 | 0.96 ± 0.26 | 0.84 |
| E226D | −59 ± 11 | 48 ± 17 | 1.0 ± 0.2 | 0.83 |
| E226Q | 144 ± 34 | 155 ± 12 | 0.40 ± 0.06 | 1.0 |
| V227E | −101 ± 15 | 67 ± 10 | 0.83 ± 0.11 | 0.97 |
| C229S | −108 ± 4 | 60.5 ± 5 | 0.84 ± 0.06 | 0.88 |
| R305E | −103 ± 4 | 56 ± 14 | 0.86 ± 0.09 | 0.84 |
| R312Q | −93 ± 9 | 40 ± 7 | 1.0 ± 0.16 | 0.69 |
| C415S | −99 ± 5 | 47.7 ± 4 | 1.0 ± 0.07 | 0.84 |
| A417F | −133 ± 16 | 78 ± 11 | 0.81 ± 0.1 | 1.09 |
| F418A | ND | ND | ND | ND |
| F418C | −64 ± 8 | 79.5 ± 2 | 0.93 ± 0.14 | 1.28 |
| V419M | −111 ± 15 | 73.6 ± 5 | 0.82 ± 0.1 | 1.04 |
| P420G | −135 ± 11 | 99 ± 13 | 0.50 ± 0.05 | 0.86 |
| H472K | ND | ND | ND | ND |
| Y512A | −80 ± 12 | 51 ± 5 | 0.81 ± 0.13 | 0.71 |
| K519Q | −103 ± 17 | 64 ± 7 | 0.96 ± 0.18 | 1.07 |

The voltage of half-maximal activation (at pH 7.3) and the apparent gating valence (z) are shown in columns 2 and 4, respectively. The slope of the $V_{1/2}$ − pH curve was obtained from a linear fit to all data points, except for mutant F214L for which the slope was obtained from $V_{1/2}$ values at pH 9.0 and 10. The last column displays the product of the slope (column 3) and the apparent gating valence (column 4), divided by 58 mV. Theoretical considerations (Boccaccio et al., 1998) indicate that this product takes into account the unspecific interdependence of these two parameters. For each mutant at least five patches were used for the averages. Error bars indicate SD; ND (not determined) indicates mutants for which the Boltzmann analysis was not possible.

block by $OH^-$ anions, similar to the voltage-dependent block of E166A by the small organic acid CPA (Traverso et al., 2003).

### Kinetic Analysis of pH Dependence of WT ClC-0 at Basic $pH_{int}$

From the mutational analysis no residue emerged that could be a good candidate as intracellular pH sensor. To obtain more insight into the mechanism of the pH dependence of the fast gate, we thus performed a detailed kinetic analysis of the fast gating relaxations. We concentrated on the basic pH range because in this range gating is determined by the major voltage-dependent process that is associated with an exponential voltage dependence of the opening and closing rate.

Fig. 5 A shows representative current traces at −140 and +140 mV (pH 9) and illustrates the monoexponential

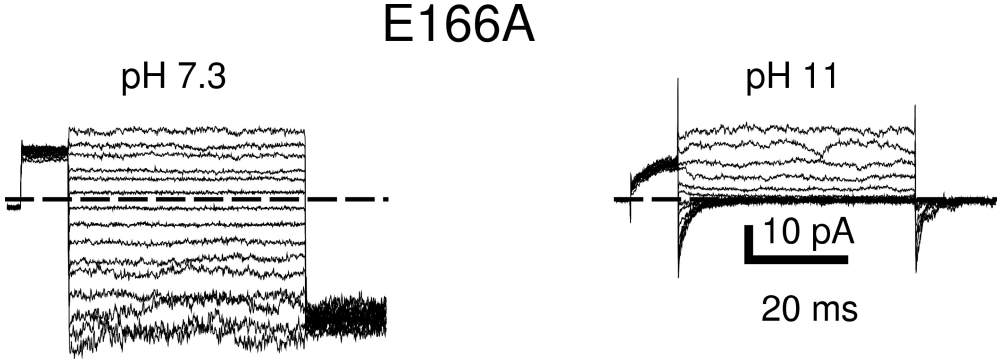


**Figure 4.** pH dependence of mutant E166A. Shown are current traces from an inside-out patch at control pH and at pH 11. Note the time-dependent current decrease at negative voltages. Similar results were obtained in two other patches.

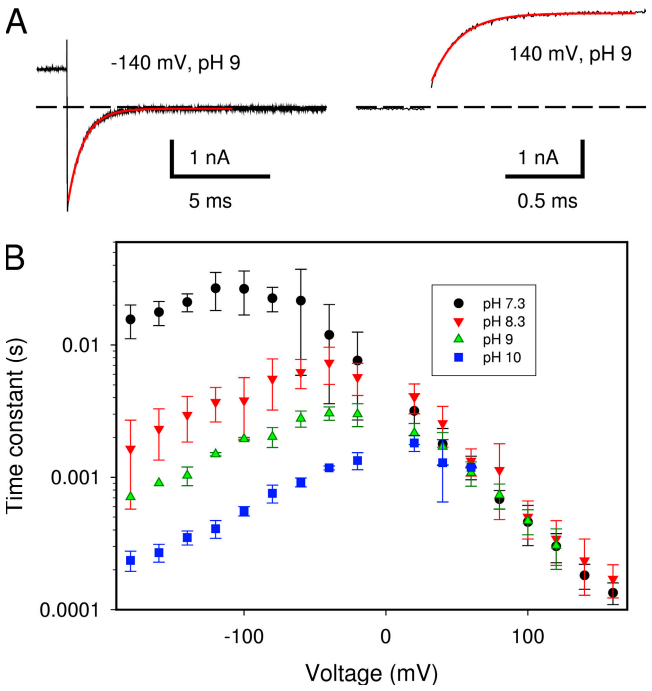


**Figure 5.** Kinetic analysis of fast gating. In A are shown typical traces (from a patch at pH 9) used for the determination of the single exponential relaxation time constants. In the right panel the capacitive transient has been blanked for clarity. Red lines are single exponential fits with $\tau = 0.79$ ms (−140 mV) and $\tau = 0.18$ ms (+140 mV). In B are plotted mean values for the time constants at various pH as a function of voltage.

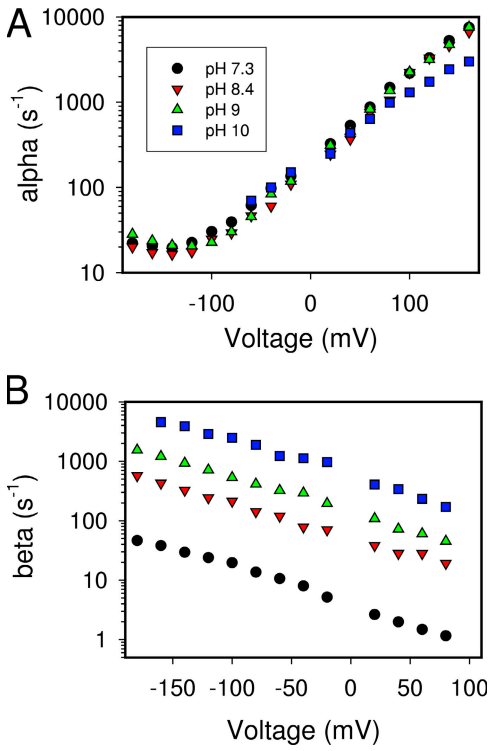


**Figure 6.** Opening and closing rate constants at different pH. From the time constants (Fig. 5) and the steady-state open probability (see Fig. 1) the opening rate constants (A) and the closing rate constants (B) were calculated according to Eq. 3. For clarity, error bars are not shown.

fit to the deactivating and activating segments of the current that were used to obtain the time constants for channel opening and channel closing. Increasing the pH from 7.3 to 10 progressively decreases the time constant up to about two orders of magnitude at negative potentials. At positive voltages, the time constants were largely pH insensitive (Fig. 5 B).

For further analysis, we exploited the fact that fast gating can be well described by a two-state process

$$C \underset{\beta}{\overset{\alpha}{\rightleftharpoons}} O$$

with a single closed state, C, and an open state, O, connected by the opening rate constant α, and the closing rate constant, β. Thus, as described earlier by others (Zhang et al., 2006; Engh et al., 2007a), we used the time constant and the apparent open probability, $p_{open}$, to obtain estimates for α and β by

$$\alpha = \frac{p_{open}}{\tau}; \beta = \frac{1 - p_{open}}{\tau}. \quad (3)$$

The resulting values are plotted in Fig. 6 as a function of voltage for the various pH values.

Intracellular pH has only very small effects on the opening rate (α) of the channel in the whole voltage range tested (from −180 to 160 mV) (Fig. 6 A).

Intracellular pH mainly affects the closing rate of the channel (β). The rate of channel closing progressively increases at negative voltages. Importantly, at all potentials tested, β increases progressively from pH 7.3 to pH 10.

### Effect of Intracellular $Cl^-$ on the pH Dependence of Fast Gating

Chen and coworkers have previously demonstrated that intracellular $Cl^-$ ions have a drastic effect on the channel closing rate with only modest effects on the channel opening rate (Chen and Miller, 1996; Chen et al., 2003). This is surprisingly similar to what we see for intracellular $H^+$; the closing rate but not the opening rate depends on $pH_{int}$. To investigate the interdependence of internal $Cl^-$ and internal pH on channel gating, we measured the (apparent) steady-state open probability and the kinetics of gating at the reduced internal $Cl^-$ concentration of 14 mM and at pH values ranging from 7.3 to 10. Typical current traces are shown in Fig. 7 A. As described above, we used the data to extract estimates for the opening rate (α) and closing rate (β) as a function of voltage and pH. Similar to what has been observed in

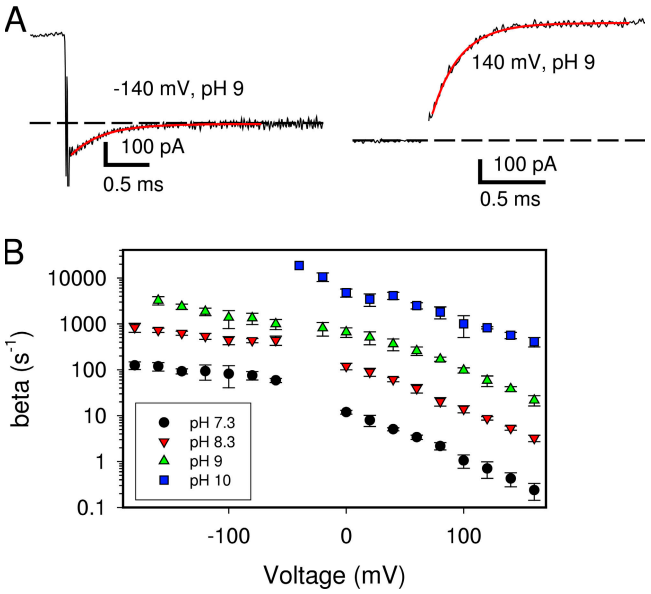


**Figure 7.** Kinetic analysis of fast gating at low (14 mM) $Cl^-_{int}$. (A) Typical traces (from a patch at pH 9) used for the determination of the single exponential relaxation time constants. In the right panel the capacitive transient has been blanked for clarity. Red lines are single exponential fits with $\tau = 0.37$ ms (−140 mV) and $\tau = 0.22$ ms (+140 mV). (B) Plots of mean values for the closing rate constant determined as in Fig. 6 at various pH as a function of voltage.

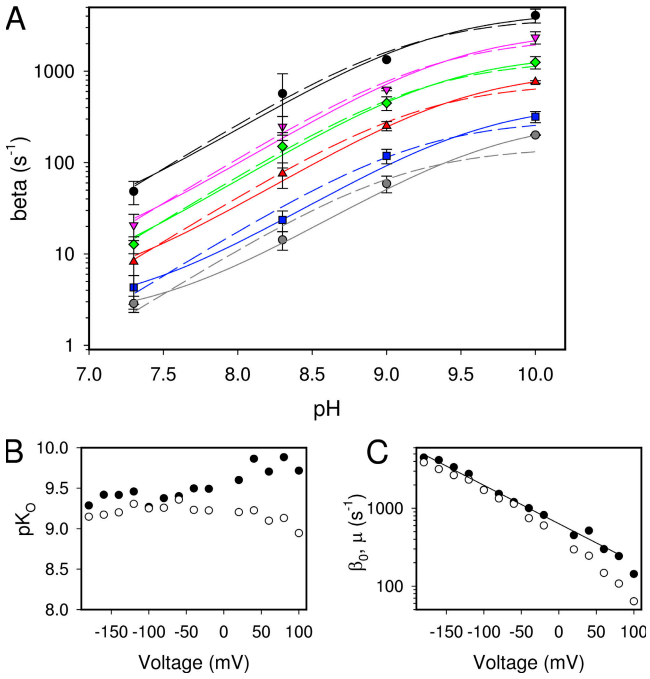


**Figure 8.** pH dependence of the closing rate constants—first models. (A) Plots of the values for the closing rate constant (same values as in Fig. 6) as a function of pH with different symbols for different voltages (for clarity, values are shown only for a few representative voltages: black circles, −180 mV; pink triangles down, −120 mV; green diamonds, −80 mV; red triangles up, −40 mV; blue squares, 20 mV; gray circles, 60 mV). Solid lines are fits of Eq. 5 with the resulting $pK_O$ and $\beta_0$ reported in B and C, respectively, as filled circles. The solid line in C is a fit of the filled circles to an exponential function of the form $\beta_0 = \beta_0(0)*\exp(z*VF/(RT))$, where F is Faradays constant, R the gas constant, T the absolute temperature, $\beta_0(0)$ the value of $\beta_0$ at 0 mV, and z the "slope" of the curve, resulting in $z = 0.28$. Dashed lines in A are fits of Eq. 7 with the resulting $pK_O$ and $\mu$ reported in B and C, respectively, as open circles.

high $Cl^-$, the closing rate (Fig. 7 B) is much more dependent on pH than the opening rate constant (not depicted). Interestingly, the dependence of β on voltage appears to deviate from a simple exponential voltage dependence at 14 mM $Cl^-$.

### A Formal Model for $pH_{int}$ Dependence of the Fast Gate

What is the mechanism by which intracellular protons modulate the fast gate? In the model that was originally proposed by Hanke and Miller (1983) the protonation state of an intracellularly accessible group modulates opening and closing transitions in an allosteric manner (Model 1):

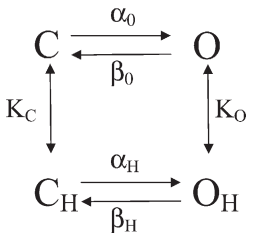


(MODEL 1)

Unprotonated channels gate with opening and closing rate constants, $\alpha_0$ and $\beta_0$, respectively, whereas protonated channels gate with rate constants $\alpha_H$ and $\beta_H$. Protonation of the closed and open state are governed by the dissociation constants $K_C$ and $K_O$, respectively (or the associated $pK_C = -\log(K_C)$ and $pK_O = -\log(K_O)$). Assuming that protonation/deprotonation is fast compared with the "gating transitions," Model 1 predicts apparent opening and closing rate constants, $\alpha_{eff}$ and $\beta_{eff}$, given by

$$\alpha_{eff} = \frac{\alpha_0 + \alpha_H H / K_C}{1 + H / K_C} \quad (4)$$

$$\beta_{eff} = \frac{\beta_0 + \beta_H H / K_O}{1 + H / K_O}, \quad (5)$$

where H denotes the $H^+$ concentration. The predictions of Model 1 can be compared with the experimental results. First, the fact that the opening rate constant is only slightly dependent on $pH_{int}$ implies that $pK_C >> 9$ and that $\alpha_H >> \alpha_0$. Otherwise, Eq. 4 would predict a pronounced pH dependence of the opening rate.

We fitted the experimental values for the closing rate constant (Fig. 8 A) with Eq. 5, with the three parameters $\beta_0$, $\beta_H$, and $K_O$ for each pH (solid lines in Fig. 8 A for example voltages). Eq. 5 is clearly adequate to describe the

experimental data and from the fit we can draw several important, general conclusions. First, the proton binding constant of the open state, $K_O$, is practically voltage independent (Fig. 8 B). Second, the resulting values for the closing rate constant of protonated channels, $\beta_H$, are small (not depicted). The closing rate constant of unprotonated channels, $\beta_0$, has an exponential voltage dependence with an apparent gating valence of z = 0.28 (Fig. 8 C), in agreement with results from Chen and Miller (1996).

Since $\alpha_0$ and $\beta_H$ are negligible, Model 1 can be formally reduced to the simpler Model 2:

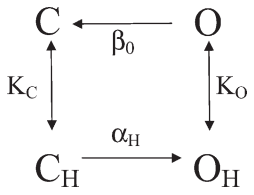


(MODEL 2)

in which opening occurs exclusively from protonated channels, whereas closing occurs only from unprotonated channels. The fact that Model 2 implies net anti-clockwise cycling and thus thermodynamic disequilibrium is uncomforting to a certain extent but probably not completely surprising given that gating of ClC-0 is known to be coupled to ion permeation process in a nonequilibrium fashion (Richard and Miller, 1990; Pusch et al., 1995; Chen and Miller, 1996).

### A Possible Mechanism of the Fast Gate Involving an $H^+$ Acceptor

Model 2 gives a formal description of the proton dependence of gating but provides relatively little insight into the molecular mechanism of how intracellular protons affect fast gating. It is well established that the conserved glutamate residue 166 is of crucial importance for fast gating. In the crystal structure of the bacterial ClC-ec1, the side chain of the homologous residue E148 blocks the exit of a bound $Cl^-$ ion toward the extracellular solution (Dutzler et al., 2002). This has led to the hypothesis that E166 acts as a "gate" in ClC-0 that has to open in order to allow ion permeation. Consistent with this idea, mutants E166A, E166Q, and E166S have a practically completely "open" phenotype: they lack voltage dependence, chloride dependence, and $pH_{ext}$ dependence (Dutzler et al., 2003; Traverso et al., 2003). Furthermore, the fast gate of ClC-0 can be similarly locked open in low $pH_{ext}$ (Chen and Chen, 2001; Dutzler et al., 2003). The latter result suggests that E166 has to be protonated in order to be removed from its "blocking" position, in agreement with theoretical investigations (Kuang et al., 2007), even though there is no direct evidence for this. Assuming, thus, that opening of the fast gate requires protonation of E166, a natural mechanism to explain the $pH_{int}$ dependence and the voltage dependence of gating is that intracellular protons reach E166 in a voltage-dependent manner (Miller, 2006; Traverso et al., 2006). The simplest scheme incorporating this idea is given by Model 3:

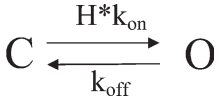


(MODEL 3)

in which direct protonation of E166 from the intracellular solution opens the channel. This model can be discarded immediately because it predicts an opening rate that is proportional to $[H^+]$ and a pH-independent closing rate, in contrast to the experimental results. Thus, similar to the Hanke and Miller model (1), at least one saturable intracellular proton acceptor must be invoked in order to describe the pH dependence of the apparent opening and closing rates. We denote the hypothetical intracellular proton acceptor by A in its deprotonated form and by AH in its protonated form. Similarly, we abbreviate the unprotonated and protonated state of Glu-166 by $E^-$, or EH, respectively. With this notation, and assuming that protonation of E166 is required for channel opening, the gating transitions can be described by the following scheme:

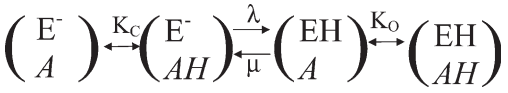


(MODEL 4)

In this scheme, we restrict our attention to the influence of intracellular protons and neglect the effect of $pH_{ext}$. Similar to Model 1 we assume fast equilibration of protons with the intracellular acceptor, governed by the equilibrium constants $K_C$ and $K_O$, respectively, depending on the protonation state of E166. The rate limiting step for opening/closing is the voltage-dependent proton transfer between the intracellular acceptor and E166, described by $\lambda$ and $\mu$, respectively. Given that states in which E166 is protonated are "open," the effective opening and closing rate constants, $\alpha_{eff}$ and $\beta_{eff}$, for Model 4 are given by

$$\alpha_{eff} = \frac{\lambda H / K_C}{1 + H / K_C} \tag{6}$$

$$\beta_{eff} = \frac{\mu}{1 + H / K_O}. \tag{7}$$

These equations are formally practically equivalent to Eqs. 4 and 5, because we could conclude that in Model 1, $\beta_H$ and $\alpha_0$ are negligible. In fact, fitting Eq. 7 to the closing rate (Fig. 8 A, dashed lines for representative voltages) results in values for $K_O$ (Fig. 8 B, open symbols) and the closing rate $\mu$ (Fig. 8 C, open symbols) very similar to the corresponding values obtained for Model 1 (Fig. 8, B and C, filled symbols).

Thus, formally, we cannot distinguish between an allosteric regulation of gating by intracellular protons and a

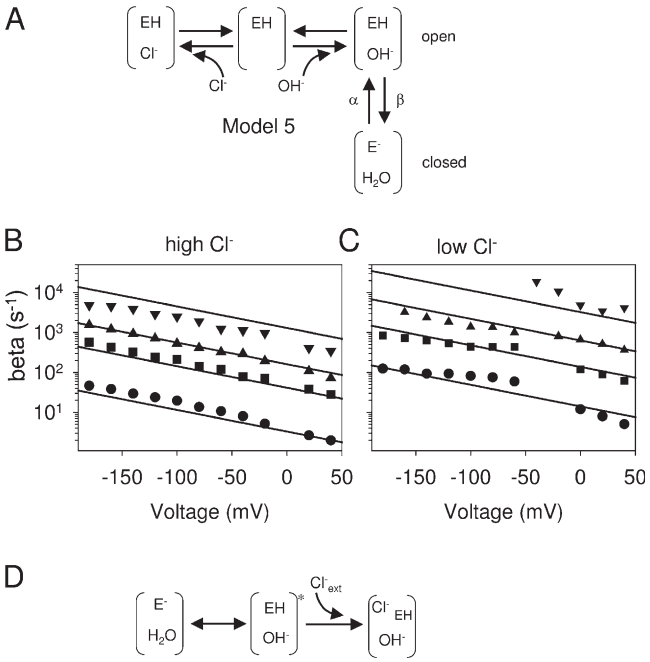


**Figure 9.** Model of pH-dependent gating of ClC-0 involving water dissociation. In A, the model is schematically drawn (see text for details). (B and C) Closing rate constants at 104 mM $Cl^-$ (B) and 14 mM $Cl^-$ (C) (data from Fig. 6 B and Fig. 7 B, respectively; circles, pH 7.3; squares, pH 8.3; triangles up, pH 9; triangles down, pH 10) together with a best fit of Eq. 8 with the following parameters: $\beta(0) = 6003\ s^{-1}$, $z\beta = 0.31$, $K_{Cl}(0) = 16.6$ mM, $K_{OH}(0) = 46\ \mu M$, $z_{Cl} = 0$. (D) A hypothetical model of how extracellular $Cl^-$ ions could facilitate gate opening. The initially protonated state (indicated by *) is metastable and requires the occupation of the external binding site by a $Cl^-$ ion for channel opening.

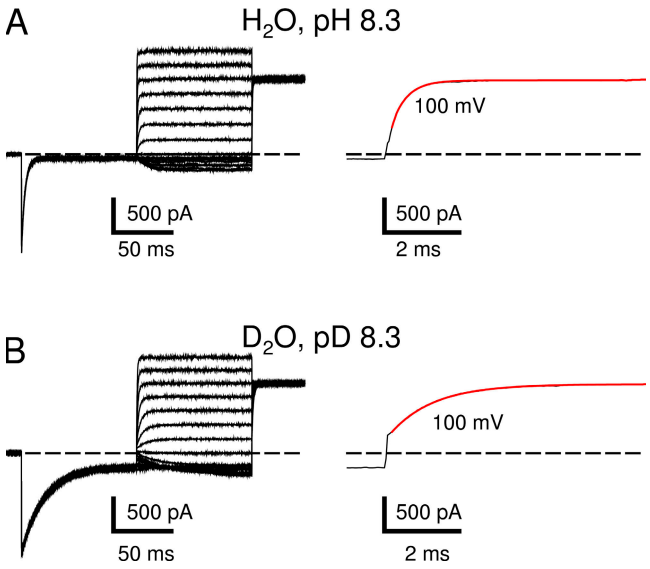


**Figure 10.** Fast gating relaxations in $D_2O$. Representative current traces from an inside out patch measured in the standard $H_2O$ solution (A) or in $D_2O$ (B) at pH/pD 8.3. The extracellular solution was in $H_2O$. The pulse protocol consisted of a prepulse to −140 mV, test pulses ranging from 140 to −160 mV, and a tail pulse to 100 mV. The right panels show a zoom of the pulses to 100 mV, superimposed with a monoexponential fit (red line).

direct protonation of E166 as the crucial gating step. Nevertheless, it is reasonable to assume that E166 needs to be protonated in order for the channel to open.

### An Alternative Mechanism of Opening—Dissociation of a Water Molecule

Even though the above described Model 4 can fit the data obtained for the closing rate, it is qualitatively inconsistent with the almost complete independence of the opening rate on pH and $[Cl^-]_{int}$ and the very strong dependence of the closing rate on these parameters. The apparent dependence of the opening rate on $pH_{int}$ described by Hanke and Miller (1983) is most likely due to the effect of $pH_{ext}$, because these authors changed pH on both sides of the membrane.

An alternative mechanism is illustrated in Fig. 9 A (Model 5). In this model, the proton required to open the channel derives from the dissociation of a water molecule. The resulting hydroxyl anion is stabilized by the positive electrostatic potential of one (or more) of the anion binding sites. Conversely, channel closing is only possible if a hydroxyl anion is bound in the channel, acting as the acceptor of the free proton dissociated from the side chain of E166. This model is in qualitative agreement with three key observations. (1) The opening rate is independent from the intracellular pH. (2) The closing rate is strongly dependent on pH. (3) The closing rate (but not the opening rate) is strongly dependent on $[Cl^-]_{int}$.

To test if the model is in quantitative agreement with our data, we parameterized the closing transitions predicted by Model 5 in the following manner, again excluding for simplicity effects of $pH_{ext}$ and $[Cl^-]_{ext}$. Intracellular $Cl^-$ and $OH^-$ ions bind competitively to a site with apparent dissociation constants given by

$$K_{Cl} = K_{Cl}(0)\exp(z_{Cl}\varphi)$$

$$K_{OH} = K_{OH}(0)\exp(z_{Cl}\varphi),$$

with $\varphi = VF/(RT)$, $z_{Cl}$ the electrical distance of the $Cl^-$ (and $OH^-$) binding site from the intracellular solution, and the respective dissociation constants $K_{Cl}(0)$ and $K_{OH}(0)$ at 0 mV. The closing rate $\beta$ (from the $OH^-$ occupied state, see Fig. 9 A) is voltage dependent with

$$\beta(V) = \beta(0)\exp(-z_\beta\varphi)$$

with the electrical distance $z_\beta$, and the closing rate $\beta(0)$ at 0 mV. Using the definitions

$$r_{Cl} = \frac{[Cl]_{int}}{K_{Cl}} = \frac{[Cl]_{int}}{K_{Cl}(0)}\exp(-z_{Cl}\varphi)$$

and

$$r_{OH} = \frac{[OH]_{int}}{K_{OH}} = \frac{[OH]_{int}}{K_{OH}(0)} \exp(-z_{Cl}\varphi)$$

the relative occupancy of the $OH^-$ bound open state is given by

$$p(OH^- bound) = \frac{r_{OH}}{1 + r_{Cl} + r_{OH}}.$$

Since channels can close only from this state with the rate constant $\beta(0)\exp(-z_\beta\varphi)$, the effective closing rate constant is thus given by

$$\beta_{eff}(V) = \beta(0)\exp(-z_\beta\varphi)\frac{r_{OH}}{1 + r_{Cl} + r_{OH}}. \qquad \text{(Eq. 8)}$$

The solid lines in Fig. 9 (B and C) show the best fit of Eq. 8 with the parameters given in the figure legend. We restricted the fit to voltages less positive than 60 mV, first because the closing rate is in principle more difficult to determine at positive voltages, and, second, because we expect the influence of extracellular $Cl^-$ on the closing rate to be larger at positive voltages. A relatively good, albeit not "perfect," agreement of the model with the data can be achieved. The resulting parameters suggest an apparent (practically voltage-independent) $K_D$ for $OH^-$ ions of 46 μM and an apparent $K_D$ for $Cl^-$ ions of 16 mM.

### Deuterium Isotope Effects on Fast Gating

If proton translocation is a rate limiting event for channel opening, a large effect of $D_2O$ substitution on the opening rate constant can be expected (DeCoursey and Cherny, 1997). To test this prediction we measured gating relaxations in $D_2O$ solutions applied to the cytoplasmic side. Typical traces are shown in Fig. 10 B, with the control of the same patch in $H_2O$ shown in Fig. 10 A, both at pH/pD 8.3. Gating relaxations are clearly slower at positive and at negative voltages in $D_2O$ compared with $H_2O$. On the other hand, external $D_2O$ had only a very small effect on gating (unpublished data). We performed a kinetic analysis as in Fig. 6 to extract the opening and closing rate constants at pD 7.3 and pD 8.3. Results are shown in Fig. 11. In $D_2O$, the opening rate constant is slowed by a factor of ~3.1 for voltages ≥ −40 mV (Fig. 11 C), independently from the pH (Fig. 11 A). The closing rate constant is affected even more drastically (Fig. 11, B and D). These results are in full agreement with the predictions of Model 5. First of all, the slowing by a factor of 3.1 is significantly larger compared with what is found for $D_2O$ modification of other ion channels not involving $H^+$ transfer reactions (for a comprehensive overview see DeCoursey and Cherny, 1997), directly supporting the view that proton transfer is involved in the opening step. Second, as explained in the Discussion, also the slowing of the closing rate constant in $D_2O$ is in nice agreement with Model 5.

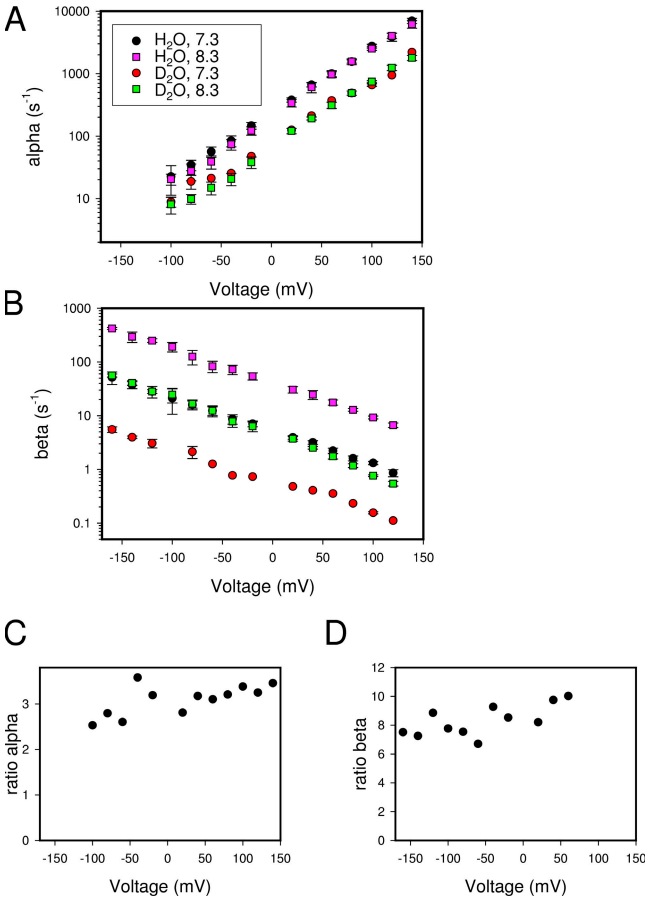


**Figure 11.** Opening and closing rate constants in $D_2O$. Opening (A) and closing (B) rate constants were determined as in Fig. 6. Since slightly different solutions were employed in these experiments (see Materials and methods), the rate constants in $H_2O$ represent the values obtained from the same patches in which we tested the effect of $D_2O$. (C) The ratio of the opening rate constants at pH/pD 8.3 in $H_2O$ and $D_2O$. (D) The ratio of the closing rate constants at pH/pD 8.3 in $H_2O$ and $D_2O$.

## DISCUSSION

The strong dependence of the fast gate of ClC-0 on protons has long been known (Hanke and Miller, 1983). A possible molecular mechanism for such an effect became evident after the structure determination of the bacterial ClC-ec1 homologue (Dutzler et al., 2002). The presumably negatively charged, i.e., deprotonated, side chain of a highly conserved glutamate residue (E148) blocked the passage of a centrally bound $Cl^-$ ion toward the extracellular space. The fundamental role of this glutamate for CLC functioning was confirmed by crystal structures in which the glutamate was neutralized; a $Cl^-$ ion was found to replace the WT E148 side chain (Dutzler et al., 2003). In addition, functional studies of ClC-0 confirmed the

critical role of the glutamate: mutational neutralization or application of low extracellular pH locked the fast gate open (Chen and Chen, 2001; Dutzler et al., 2003; Traverso et al., 2003). The role of protons for CLC functioning became even more prominent and interesting with the surprising discovery that the bacterial ClC-ec1 and several eukaryotic CLC proteins are actually not passive $Cl^-$ ion channels but secondary active, strictly coupled, and electrogenic $Cl^-/H^+$ antiporters (Accardi and Miller, 2004; Picollo and Pusch, 2005; Scheel et al., 2005; De Angeli et al., 2006; Nguitragool and Miller, 2006). Thus, a reasonable hypothesis is that the proton dependence of ClC-0 and other CLC channels is mechanistically related to the proton transport of CLC exchangers (Miller, 2006). In particular, we have recently advanced the hypothesis that most of the voltage dependence of the fast gate derives from a voltage-dependent transfer of protons form the intracellular solution to the "gating" glutamate, E166 (Traverso et al., 2006). In the present paper, we sought to decipher the mechanism of intracellular proton dependence in more detail. First, we performed a mutational analysis in order to identify a hypothetical intracellular proton acceptor. A similar approach had led to the identification of the off-pore glutamate E203 in the bacterial ClC-ec1 as a good candidate for an intracellular $H^+$ acceptor (Accardi et al., 2005). The importance of this residue for proton transport was confirmed also for ClC-4 and ClC-5 (Zdebik et al., 2008). However, the analogous residue is a valine in all known CLC channels (Accardi et al., 2005). None of the 22 residues tested in our screen turned out to be a good candidate $H^+$ acceptor. The only mutants that had a drastic effect on $pH_{int}$ sensitivity were E166A, F214L, and F418A. The insensitivity of E166A (at least for pH < 9) can be considered trivial, since the mutant is locked open anyway. In fact, we believe that the voltage and time-dependent reduction of E166A-mediated currents at pH ≥ 9 is caused by a voltage-dependent block of the mutant by $OH^-$ anions, similar to the block of the mutant by intracellular CPA (Traverso et al., 2003).

Even if we cannot exclude that other residues, not tested in this study, might act as a proton acceptor, the mutagenesis results are consistent with the idea that proton regulation of gating does not involve such an element.

To get more insight into the mechanism of proton regulation we performed a detailed kinetic analysis of channel gating. Our results are grossly compatible with three conceptually different kinds of models, posing specific constraints for each of these. The first class of models assumes an allosteric regulation of fast gating by an intracellular proton acceptor (Hanke and Miller, 1983). In the second class of models, delivery of protons from this hypothetical proton acceptor to Glu-166 directly opens the channel in a voltage-dependent manner. Both models suffer from the qualitative inconsistency with the experimentally found pH independence of the opening rate, they do not explain in an obvious way the dependence of the rate constants on $[Cl]_{int}$, and we were unable to identify the pH sensor using mutagenesis. None of these arguments is fully stringent, and we can thus not exclude those models. Nevertheless, the alternative mechanism illustrated in Fig. 9 based on water dissociation is in qualitative agreement with the dependence of the rate constants on $[Cl^-]_{int}$ and $pH_{int}$; open channels are stabilized by intracellular chloride by direct competition with hydroxyl anions, leading to a chloride dependence of the closing rate constant. Also the pH dependence of the closing rate and the pH independence of the opening rate are in natural agreement with the model shown in Fig. 9.

Strong support for the kinetic model shown in Fig. 9 was provided by the $D_2O$ substitution experiments. The opening rate constant was more than threefold smaller in $D_2O$ compared with $H_2O$. In contrast, for many other channel types, gating time constants are affected only by a factor <2 (see Table III in DeCoursey and Cherny, 1997) in $D_2O$ substitution experiments. Thus, a protonation reaction most likely represents the rate limiting step in channel opening. Also the effect of $D_2O$ substitution on the closing rate constant is in full agreement with the model shown in Fig. 9. The dissociation constant of $D_2O$ is significantly smaller than that for water ($0.14 \times 10^{-14}$ $M^2$ compared with $1.0 \times 10^{-14}$ $M^2$) (Glasoe and Long, 1960). Thus at equivalent pH/pD values, the $OD^-$ concentration is about sevenfold lower in $D_2O$ than the $OH^-$ concentration in $H_2O$. According to Model 5, the closing rate constant is not directly related to the $H^+/D^+$ concentration, but rather to the $OH^-/OD^-$ concentration. Thus, the 7–10-fold slowing of channel closure seen in $D_2O$ (Fig. 11 D) can be mostly attributed to a reduced $OD^-$ concentration.

How realistic is the possibility that protons are delivered by water dissociation? Kasianowicz et al. (1987) argue that dissociation of water is the fastest mechanism by which protons can be delivered to a membrane-associated weak acid. Also in general base catalysis, protons can be generated by water dissociation.

It should be noted that our model implies that the structure of the closed state of ClC-0 must be different from the structure of the closed conformation of ClC-ec1 (Dutzler et al., 2003). In the bacterial transporter, a completely dehydrated $Cl^-$ ion is bound in the central $Cl^-$ binding site. Water molecules, acting as proton donors, could not easily access that site.

Another important element that has to be considered in a model of the fast gate is the dependence on extracellular $Cl^-$. Previous studies have shown that the apparent open probability and, in particular, the opening rate constant, α, of the fast gate strongly depend on the extracellular $Cl^-$ concentration (Pusch et al., 1995; Chen and Miller, 1996). It was concluded that the voltage dependence of opening arises from voltage-dependent $Cl^-$ binding (Pusch et al., 1995) or a voltage-dependent

translocation of $Cl^-$ through the channel during the opening process (Chen and Miller, 1996). Recently, Engh et al. (2007a) explored in detail the extracellular $Cl^-$ dependence of the fast gate of ClC-0. From the very thorough analysis of Engh et al. it emerged that it is extremely difficult to distinguish if the voltage dependence of α arises from a voltage-dependent $Cl^-$ binding or from the voltage dependence of a subsequent "gating step," which may or may not involve $Cl^-$ translocation. In any case, a fundamental difference of the previous "$Cl^-$-dependent" gating models (Pusch et al., 1995; Chen and Miller, 1996; Dutzler et al., 2003; Engh et al., 2007a) and our proton-dependent model lies in the mechanism of how the presumably negatively charged side chain of E166 is removed from its blocking position in the closed state. The $Cl^-$-dependent gating models assume that $Cl^-$ competes with E166. Our proton-dependent model, instead, assumes that E166 has to be protonated in order to allow channel opening. Similar to the difficulty in explaining the pH dependence, none of the models are able to explain all of the data concerning the extracellular $Cl^-$ dependence. A speculative possibility of how extracellular chloride ions could influence channel opening in our proton-dependent model is illustrated in Fig. 9 D; the initial protonated state (Fig. 9 D, middle state) is metastable and requires the occupation of the external site by a $Cl^-$ ion from the extracellular space for stabilization. Clearly, much more experimental effort has to be invested in order to obtain a molecular understanding of the intricate physico chemistry of CLC channels. It is even more obscure how the pH-dependent gating of ClC-0 is related to the $Cl^-$/ $H^+$ antiport of ClC-5 or ClC-ec1. In these transporters, protons are probably taken up from the intracellular solution by E203 in ClC-ec1 (and E268 in ClC-5) and transferred to the gating glutamate via a route that does dot coincide with the chloride pathway (Accardi et al., 2005). The role of E268 as a proton transfer residue in ClC-5 was also confirmed by the finding that function was partially retained when it was exchanged by other titratable residues (e.g., histidine) but not other amino acids (Zdebik et al., 2008). Therefore, water dissociation is probably not involved in the delivery of protons from the intracellular solution in these $Cl^-/H^+$ antiporters. Future experiments, on CLC channels and CLC transporters, will help to uncover the mechanistic details of $H^+$-mediated gating and $Cl^-/H^+$ flux coupling.

We thank G. Gaggero for help in constructing the perfusion system. We also thank one of the reviewers for suggesting the $D_2O$ substitution experiments.

The financial support by Telethon Italy (grant GGP04018) is gratefully acknowledged.

Olaf S. Andersen served as editor.

Submitted: 13 March 2008
Accepted: 11 June 2008

## REFERENCES

Accardi, A., and M. Pusch. 2003. Conformational changes in the pore of CLC-0. *J. Gen. Physiol.* 122:277–293.

Accardi, A., and C. Miller. 2004. Secondary active transport mediated by a prokaryotic homologue of ClC $Cl^-$ channels. *Nature.* 427:803–807.

Accardi, A., L. Kolmakova-Partensky, C. Williams, and C. Miller. 2004. Ionic currents mediated by a prokaryotic homologue of CLC $Cl^-$ channels. *J. Gen. Physiol.* 123:109–119.

Accardi, A., M. Walden, W. Nguitragool, H. Jayaram, C. Williams, and C. Miller. 2005. Separate ion pathways in a $Cl^-/H^+$ exchanger. *J. Gen. Physiol.* 126:563–570.

Adam, Y., N. Tayer, D. Rotem, G. Schreiber, and S. Schuldiner. 2007. The fast release of sticky protons: kinetics of substrate binding and proton release in a multidrug transporter. *Proc. Natl. Acad. Sci. USA.* 104:17989–17994.

Bisset, D., B. Corry, and S.H. Chung. 2005. The fast gating mechanism in ClC-0 channels. *Biophys. J.* 89:179–186.

Boccaccio, A., O. Moran, and F. Conti. 1998. Calcium dependent shifts of $Na^+$ channel activation correlated with the state dependence of calcium-binding to the pore. *Eur. Biophys. J.* 27:558–566.

Chen, M.F., and T.Y. Chen. 2001. Different fast-gate regulation by external $Cl^-$ and $H^+$ of the muscle-type ClC chloride channels. *J. Gen. Physiol.* 118:23–32.

Chen, M.F., and T.Y. Chen. 2003. Side-chain charge effects and conductance determinants in the pore of ClC-0 chloride channels. *J. Gen. Physiol.* 122:133–145.

Chen, T.Y. 2005. Structure and function of CLC channels. *Annu. Rev. Physiol.* 67:809–839.

Chen, T.Y., and C. Miller. 1996. Nonequilibrium gating and voltage dependence of the ClC-0 $Cl^-$ channel. *J. Gen. Physiol.* 108:237–250.

Chen, T.Y., M.F. Chen, and C.W. Lin. 2003. Electrostatic control and chloride regulation of the fast gating of ClC-0 chloride channels. *J. Gen. Physiol.* 122:641–651.

De Angeli, A., D. Monachello, G. Ephritikhine, J.M. Frachisse, S. Thomine, F. Gambale, and H. Barbier-Brygoo. 2006. The nitrate/proton antiporter AtCLCa mediates nitrate accumulation in plant vacuoles. *Nature.* 442:939–942.

DeCoursey, T.E., and V.V. Cherny. 1997. Deuterium isotope effects on permeation and gating of proton channels in rat alveolar epithelium. *J. Gen. Physiol.* 109:415–434.

Dutzler, R., E.B. Campbell, M. Cadene, B.T. Chait, and R. MacKinnon. 2002. X-ray structure of a ClC chloride channel at 3.0 Å reveals the molecular basis of anion selectivity. *Nature.* 415:287–294.

Dutzler, R., E.B. Campbell, and R. MacKinnon. 2003. Gating the selectivity filter in ClC chloride channels. *Science.* 300:108–112.

Engh, A.M., and M. Maduke. 2005. Cysteine accessibility in ClC-0 supports conservation of the ClC intracellular vestibule. *J. Gen. Physiol.* 125:601–617.

Engh, A.M., J.D. Faraldo-Gomez, and M. Maduke. 2007a. The mechanism of fast-gate opening in ClC-0. *J. Gen. Physiol.* 130:335–349.

Engh, A.M., J.D. Faraldo-Gomez, and M. Maduke. 2007b. The role of a conserved lysine in chloride- and voltage-dependent ClC-0 fast gating. *J. Gen. Physiol.* 130:351–363.

Estévez, R., B.C. Schroeder, A. Accardi, T.J. Jentsch, and M. Pusch. 2003. Conservation of chloride channel structure revealed by an inhibitor binding site in ClC-1. *Neuron.* 38:47–59.

Glasoe, P.K., and F.A. Long. 1960. Use of glass electrodes to measure acidities in deuterium oxide. *J. Phys. Chem.* 64:188–189.

Hanke, W., and C. Miller. 1983. Single chloride channels from *Torpedo* electroplax. Activation by protons. *J. Gen. Physiol.* 82:25–45.

Jentsch, T.J. 2008. CLC chloride channels and transporters: from genes to protein structure, pathology and physiology. *Crit. Rev. Biochem. Mol. Biol.* 43:3–36.

Jentsch, T.J., K. Steinmeyer, and G. Schwarz. 1990. Primary structure of *Torpedo marmorata* chloride channel isolated by expression cloning in *Xenopus* oocytes. *Nature.* 348:510–514.

Jentsch, T.J., V. Stein, F. Weinreich, and A.A. Zdebik. 2002. Molecular structure and physiological function of chloride channels. *Physiol. Rev.* 82:503–568.

Jentsch, T.J., I. Neagoe, and O. Scheel. 2005a. CLC chloride channels and transporters. *Curr. Opin. Neurobiol.* 15:319–325.

Jentsch, T.J., M. Poet, J.C. Fuhrmann, and A.A. Zdebik. 2005b. Physiological functions of CLC Cl channels gleaned from human genetic disease and mouse models. *Annu. Rev. Physiol.* 67:779–807.

Kasianowicz, J., R. Benz, and S. McLaughlin. 1987. How do protons cross the membrane-solution interface? Kinetic studies on bilayer membranes exposed to the protonophore S-13 (5-chloro-3-tert-butyl-2'-chloro-4' nitrosalicylanilide). *J. Membr. Biol.* 95:73–89.

Kuang, Z., U. Mahankali, and T.L. Beck. 2007. Proton pathways and $H^+/Cl^-$ stoichiometry in bacterial chloride transporters. *Proteins.* 68:26–33.

Lin, C.W., and T.Y. Chen. 2003. Probing the pore of ClC-0 by substituted cysteine accessibility method using methane thiosulfonate reagents. *J. Gen. Physiol.* 122:147–159.

Lin, Y.W., C.W. Lin, and T.Y. Chen. 1999. Elimination of the slow gating of ClC-0 chloride channel by a point mutation. *J. Gen. Physiol.* 114:1–12.

Lorenz, C., M. Pusch, and T.J. Jentsch. 1996. Heteromultimeric CLC chloride channels with novel properties. *Proc. Natl. Acad. Sci. USA.* 93:13362–13366.

Ludewig, U., T.J. Jentsch, and M. Pusch. 1997a. Analysis of a protein region involved in permeation and gating of the voltage-gated *Torpedo* chloride channel ClC-0. *J. Physiol.* 498:691–702.

Ludewig, U., T.J. Jentsch, and M. Pusch. 1997b. Inward rectification in ClC-0 chloride channels caused by mutations in several protein regions. *J. Gen. Physiol.* 110:165–171.

Matulef, K., and M. Maduke. 2007. The CLC 'chloride channel' family: revelations from prokaryotes. *Mol. Membr. Biol.* 24:342–350.

Miller, C. 2006. ClC chloride channels viewed through a transporter lens. *Nature.* 440:484–489.

Miller, C., and M.M. White. 1980. A voltage-dependent chloride conductance channel from *Torpedo* electroplax membrane. *Ann. N. Y. Acad. Sci.* 341:534–551.

Nguitragool, W., and C. Miller. 2006. Uncoupling of a CLC $Cl^-/H^+$ exchange transporter by polyatomic anions. *J. Mol. Biol.* 362:682–690.

Picollo, A., and M. Pusch. 2005. Chloride/proton antiporter activity of mammalian CLC proteins ClC-4 and ClC-5. *Nature.* 436:420–423.

Pusch, M. 1996. Knocking on channel's door. The permeating chloride ion acts as the gating charge in ClC-0. *J. Gen. Physiol.* 108:233–236.

Pusch, M. 2004. Structural insights into chloride and proton-mediated gating of CLC chloride channels. *Biochemistry.* 43:1135–1144.

Pusch, M., U. Ludewig, A. Rehfeldt, and T.J. Jentsch. 1995. Gating of the voltage-dependent chloride channel CIC-0 by the permeant anion. *Nature.* 373:527–531.

Pusch, M., A. Liantonio, L. Bertorello, A. Accardi, A. De Luca, S. Pierno, V. Tortorella, and D.C. Camerino. 2000. Pharmacological characterization of chloride channels belonging to the ClC family by the use of chiral clofibric acid derivatives. *Mol. Pharmacol.* 58:498–507.

Richard, E.A., and C. Miller. 1990. Steady-state coupling of ion-channel conformations to a transmembrane ion gradient. *Science.* 247:1208–1210.

Rychkov, G.Y., D.S. Astill, B. Bennetts, B.P. Hughes, A.H. Bretag, and M.L. Roberts. 1997. pH-dependent interactions of $Cd^{2+}$ and a carboxylate blocker with the rat ClC-1 chloride channel and its R304E mutant in the Sf-9 insect cell line. *J. Physiol.* 501:355–362.

Scheel, O., A.A. Zdebik, S. Lourdel, and T.J. Jentsch. 2005. Voltage-dependent electrogenic chloride/proton exchange by endosomal CLC proteins. *Nature.* 436:424–427.

Traverso, S., L. Elia, and M. Pusch. 2003. Gating competence of constitutively open CLC-0 mutants revealed by the interaction with a small organic Inhibitor. *J. Gen. Physiol.* 122:295–306.

Traverso, S., G. Zifarelli, R. Aiello, and M. Pusch. 2006. Proton sensing of CLC-0 mutant E166D. *J. Gen. Physiol.* 127:51–66.

Zdebik, A.A., G. Zifarelli, E.Y. Bergsdorf, P. Soliani, O. Scheel, T.J. Jentsch, and M. Pusch. 2008. Determinants of anion-proton coupling in mammalian endosomal CLC proteins. *J. Biol. Chem.* 283:4219–4227.

Zhang, X.D., Y. Li, W.P. Yu, and T.Y. Chen. 2006. Roles of K149, G352, and H401 in the channel functions of ClC-0: testing the predictions from theoretical calculations. *J. Gen. Physiol.* 127:435–447.

Zifarelli, G., and M. Pusch. 2007. CLC chloride channels and transporters: a biophysical and physiological perspective. *Rev. Physiol. Biochem. Pharmacol.* 158:23–76.